The slowly formed Guiselin brush

B. O'SHAUGHNESSY and D. VAVYLONIS

Department of Chemical Engineering, Columbia University - New York, NY 10027, USA

Abstract. – We study polymer layers formed by irreversible adsorption from a polymer melt. Our theory describes an experiment which is a "slow" version of that proposed by Guiselin (*Europhys. Lett.*, **17** (1992) 225) who considered instantaneously irreversibly adsorbing chains and predicted a universal density profile of the layer after swelling with solvent to produce the "Guiselin brush". Here we ask what happens when adsorption is *not* instantaneous. The classic example is chemisorption. In this case the brush is formed slowly and the final structure depends on the experiment's duration, t_{final}. We find the swollen layer consists of an inner region of thickness $z^* \sim t_{\text{final}}^{-5/3}$ with approximately constant density and an outer region extending up to height $h \sim N^{5/6}$ which has the same density decay $\sim z^{-2/5}$ as for the Guiselin case.

Introduction. – Several years ago, Guiselin [1] proposed an experiment to study irreversible polymer adsorption. In its simplest form, a melt is exposed to a surface so attractive to the polymer chains that they adsorb instantaneously and irreversibly. This freezes in melt chain configurations, including the size distribution of surface loops (see fig. 1(a)). The adsorbed layer is then swollen with solvent, washing away unattached chains. Guiselin predicted that the resulting interfacial structure, which has come to be known as the "Guiselin brush", has a universal density profile, $c(z) \sim z^{-2/5}$ in good solvent. Neutron scattering [2,3] and neutron reflectivity [4,5] studies have indicated density profiles both consistent [3,5] and inconsistent [4] with this prediction.

In this letter we study the same irreversible melt adsorption processes as did Guiselin, but we ask: what replaces the Guiselin brush if the adsorption is *not* instantaneous? The most important example of this is *chemisorption* where functionalized chains develop polymer-surface bonds which are usually irreversible. This arises in various technologies where polymers are attached to solid surfaces to permanently modify surface properties [6–8] (fig. 1(a)). For example, in fiber-reinforced thermoplastics, strong polymer-fiber interfaces are frequently created by chemisorption of polymers onto the fibers after functionalization of fiber surfaces with coupling agents [8–10]. Another related class involves reinforcement of immiscible polymer interfaces by chemical reactions between multi-functionalized chains at the interfaces [11].

Unlike the physisorption processes studied by Guiselin, chemisorption is extremely slow (microscopically speaking) in that 2 mutually reactive groups must collide millions of times,
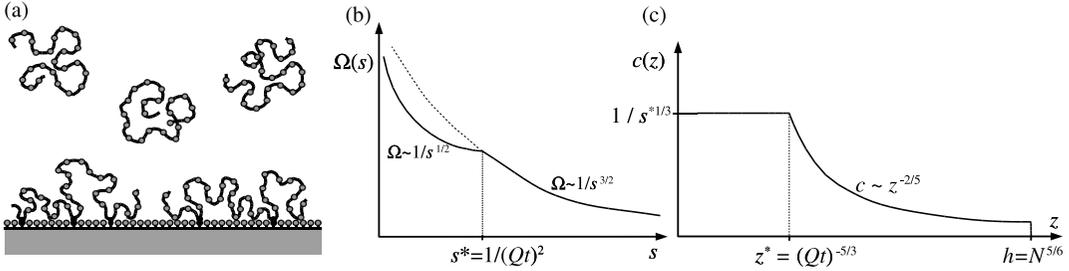
Fig. 1 – (a) Schematic of polymer melt containing reactive chains in contact with a functionalised surface. As reactions proceed, irreversible bonds form (black groups) and a layer consisting of loops and tails develops. Experimentally the degree of polymer functionalization, f, and fraction of reactive chains, X, can be varied (here we mainly consider $f = X = 1$). Bond formation is slow and requires a very large number of monomer-surface collisions. (b) Distribution of chemisorbed loop sizes after time t. Loops smaller than $s^*(t) \approx 1/(Qt)^2$ descend unhindered by others and follow the free-chain power law $\Omega_t \sim s^{-1/2}$. The distribution of big loops ($s > s^*(t)$) is frozen in time, $\Omega_t \sim s^{-3/2}$. Total grafting density $\approx 1/s^{*1/2}$. As time proceeds the dividing line shifts to the left and the future distribution is shown (dotted line). For a given loop size $s < s^*(t)$, the density will continue to grow until the critical value is reached and then halt. If uninterrupted the final loop distribution, a single $s^{-3/2}$ power, is reached after $t \approx Q^{-1}$. (c) Density profile of the swollen chemisorbed layer. The profile exhibits two regions, separated by $z = z^*$. The inner region has approximately constant density while the density in the outer region decays as $z^{-2/5}$. The longer the melt chemisorption is allowed to persist, the thinner the inner region. For experimental times exceeding Q^{-1} it shrinks to zero.

typically, before bonding [12]. Hence surface loops usually have time to explore all configurations before further reactions constrain their motion. As we will see, this leads to a different surface loop structure and a modified version of the Guiselin brush after solvent swelling.

Due to screening, polymer melt statistics are ideal. Now the probability that a random walk originating from a surface never re-contacts that surface after s steps is $\sim 1/s^{1/2}$. Its derivative gives the surface loop distribution $\omega(s) \sim 1/s^{3/2}$ in a melt. In Guiselin's experiment this is instantaneously frozen in. To see why slow chemisorption produces different $\omega(s)$, consider first an unentangled melt of chains each comprising N chemically reactive units. Chains within a coil radius $N^{1/2}$ of the surface make many surface contacts (taking monomer size as unity). Now reactions are switched on and the surface density (per site of size unity) of bonded monomers, $\Gamma_{\text{bound}}(t)$, starts increasing from zero. After time τ_N, of order-1 polymer-surface bonds per chain in this slab will have been created, *i.e.*

$$\Gamma_{\text{bound}}(\tau_N) \approx 1/N^{1/2}, \quad \tau_N = 1/(QN^{1/2}). \tag{1}$$

Here Q is the local reaction rate *given* a polymer group contacts a surface site (all of which are assumed reactive for simplicity). Equation (1) equates the reacted fraction of surface sites, $Q\tau_N \ll 1$, to the number of chains per site in the slab, $1/N^{1/2}$.

Single-chain adsorption: early stages. – At this stage the slab contains surface-grafted loops (and tails) of length $\approx N$. Let us follow how one of these mother loops gradually adsorbs down onto the surface (tails behave similarly) from the moment of its creation. To begin, we ignore interference from other chains. Because Q is small, the reaction rate of the loop's s-th unit is proportional to its equilibrium surface contact probability. For small s, this is independent of N,

$$k(s \mid N) \longrightarrow k(s) \approx Q/s^{1/2} \quad (s \ll N). \tag{2}$$

Hence the loop lifetime, the inverse of its total reaction rate $\mathcal{R}_{\text{total}} \approx \int_1^N \mathrm{d}s\, k(s \mid N)$, is identified with τ_N of eq. (1). The loop evolution kinetics are [13–15]

$$\dot{\omega}_t(s) = 2 \int_s^N \mathrm{d}s'\, k(s \mid s')\omega_t(s') - \omega_t(s) \int_0^s \mathrm{d}s'\, k(s' \mid s). \tag{3}$$

In this section t denotes time after the mother loop was created, and ω_t describes an ensemble of mother loops plus daughters. For small times, $t \ll \tau_N$, to leading order there is just the single mother loop, $\omega_t(s) \approx \delta(s - N)$. Substitution into the first term in eq. (3), describing creation of s-loops, immediately gives

$$\omega_t(s) = Qt/s^{1/2}, \qquad D^<(s) = t/\tau_s, \quad \tau_s = 1/\left(Qs^{1/2}\right) \quad (s \ll N), \tag{4}$$

where τ_s is the lifetime of an s-loop. Note that the number of loops shorter than s, $D^<(s) \equiv \int_0^s \omega_t$, is very small since $t \ll \tau_N \ll \tau_s$ for these small loops. We conclude that in addition to the single mother N-loop there are of order t/τ_N smaller loops following a $1/s^{1/2}$ power law, distinct from the $3/2$ decay in the fast Guiselin brush. Note our argument neglected the second (loop loss) term: substituting the power law into eq. (3), one finds it is self-consistently much smaller (of relative order t/τ_s) than the source term.

Single-chain adsorption: collapse. – For times greater than its lifetime τ_N, the mother loop will have come down, spawning 2 daughter loops each of size $\approx N/2$, since the total reaction rate $\mathcal{R}_{\text{total}}$ is dominated by s of order N. The daughters will in turn spawn 2 roughly equal granddaughters, and so on. As this process iterates itself, more and more loops are generated; the characteristic size after time t is $s^* = 1/(Qt)^2$. Bigger loops, $s > s^*$, have already come down ($\tau_s < t$) whereas smaller loops have yet to be created ($\tau_s > t$). We can think of the mother as having multiplied into $L(t) = N/s^* \sim t^2$ offspring of equal size s^*.

For much smaller loops, the source term in the kinetics equation (3) is now dominated by $s' \approx s^*$ and gives $\dot{\omega}_t(s) \approx k(s) \int_s^\infty \mathrm{d}s'\, \omega_t(s') \approx k(s)L(t)$. Thus the loop distribution is

$$\omega_t(s \ll s^*) \approx \frac{L(t)}{s^*}\left(\frac{s^*}{s}\right)^{1/2}, \quad \omega_t(s \gg s^*) \longrightarrow 0. \tag{5}$$

We refer the reader to ref. [14] for detailed analysis of the kinetics, eq. (3), which are able to justify the simple arguments presented here. These kinetics do indeed produce a distribution with the above features, *i.e.* sharply cut off above s^* and with $1/s^{1/2}$ behaviour for small s. The crucial point is that single-loop adsorption is a *homogeneous collapse* in which all parts of the mother loop come down essentially at the same time. Generally, the class of adsorption kinetics is governed by the contact exponent θ where $k(s) \sim s^{-\theta}$. Three classes are identified in refs. [13,16]: zipping, for $\theta > 2$; accelerated zipping for $1 < \theta < 2$; and homogeneous collapse, for $\theta < 1$. The present case, $\theta = 1/2$, is collapse; because $k(s)$ decays slowly, adsorption kinetics are dominated by distant units of order the current loop size.

Many-chains. – Our single-chain collapse description neglects interference from other chains, appropriate when only a small fraction of chains are reactive. However, when all chains simultaneously attempt to collapse as in the present situation, grafted loop surface densities rapidly reach criticality. Quite generally, the critical density for a given loop size s is

$$D_{\text{crit}}^>(s) = 1/s^{1/2} \tag{6}$$

per site. Here $D_{\text{crit}}^>(s)$ counts loops equal to or bigger than s, all of which contribute chain segments of length s to the density. At the critical level their combined total mass (s per
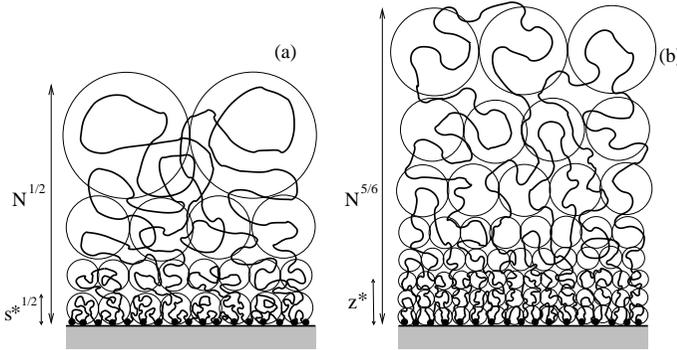
Fig. 2 – (a) Hierarchical loop structure of the adsorbed layer in the melt. Successive loop size scales are frozen in as their critical density is reached. Beyond this their formation would force chain stretching and hence is strongly suppressed. (b) Blob structure of the layer swollen in good solvent. Blob size is fixed $\approx z^{*3/10}$ in the inner region and increases as $z^{3/10}$ in the outer layer.

loop or strand) just fills a layer of thickness $s^{1/2}$, the equilibrium size. At higher densities the loops are stretched.

Returning to the many chain collapse issue, if all $1/N^{1/2}$ mother loops per site were able to collapse unhindered, each would generate N/s^* loops of size s^* by time t, giving a net density $\approx N^{1/2}/s^*$. But since this exceeds the critical level, $1/s^{*1/2}$, it is clear the unhindered collapse costs energy and must have been interfered with.

What then is the form of the loop distribution per site $\Omega_t(s)$ at time t? To proceed, we make the following assumptions: i) At time t, loops of size $s^*(t)$ are created on the surface up to the critical density and no further, ii) sizes greater than $s^*(t)$ follow a power law distribution and iii) this distribution is frozen in time. Assumptions i), iii) state that when enough time has elapsed for a certain loop size to have been created, creation of these loops proceeds, but is then permanently switched off as soon as other chains in the layer are forced to stretch to accommodate further such loops. Thus, equating $\int_{s^*}^{N} \mathrm{d}s\, \Omega_t(s)$ to $D^{>}_{\mathrm{crit}}(s^*)$ determines $\Omega \approx 1/s^{3/2}$ for all $s > s^*$ (self-consistently, the integral's lower limit dominates).

Smaller loops, $s \ll s^*(t)$, follow a different power law. From our single-chain analysis we know these are unlikely to have been created by time t even without interference and must therefore be very dilute. For these, we can essentially repeat the single-chain arguments: eq. (3) (again dominated by the source term) leads to $\dot{\Omega}_t \approx k(s)\Gamma_{\mathrm{bound}}(t)$ where the total density of loops $\Gamma_{\mathrm{bound}}(t) \approx 1/s^{*1/2}(t)$ is dominated by s^*. The crucial point is that smaller loops are sub-critical and follow free single-chain kinetics, $k(s \mid s^*) \approx k(s)$. Their distribution thus follows the single-chain power law $\Omega_t(s) \sim k(s) \sim 1/s^{1/2}$. Demanding continuity at s^* the overall layer distribution, shown in fig. 1(b), is

$$\Omega_t(s) \approx \begin{cases} cs^{-3/2}, & s^*(t) < s < N, \\ (c'/s^*(t))s^{-1/2}, & s < s^*(t), \end{cases} \qquad (7)$$

where c, c' are constants of order unity. From eq. (7) the total density of loops bigger than s is $D^{>}(s) \approx 1/s^{*1/2}(t)$ for any small loop size $s < s^*$. This confirms that such loops are sub-critical, an important self-consistency check. A sketch of the adsorbed layer loop structure is shown in fig. 2(a), characterised by a hierarchy of successively smaller loops frozen in as they reach criticality.

Guiselin experiment: swelling layer with solvent. – Let us now ask what would happen in a Guiselin-type experiment, where the chemisorption is interrupted after some time t_{final} and the brush subsequently swollen with good swelling solvent. Typical values of Q are in the range [16] $10^{-3} \lesssim Q \lesssim 10^2\,\text{s}^{-1}$, so surface saturation may not be reached for minutes or hours. After interruption, the loop distribution is frozen into the form given by eq. (7). Neglecting distinctions between tails and loops [17], after solvent is introduced the "Guiselin brush" structure is that of a polydisperse brush having chain length distribution $\Omega_t(s)$ evaluated at $t = t_{\text{final}}$.

In ref. [1], the density profile of such polydisperse grafted layers was analysed, starting from the concept of a local blob size [18] $\xi(z)$ at height z determined by the local chain grafting density $\rho(z) = 1/\xi^2(z)$. The coarse-grained chain stretching is $\text{d}z/\text{d}s \approx \xi/g$, where there are $g = \xi^{5/3}$ units per blob and the density profile is $c(z) = \rho\,\text{d}s/\text{d}z$. The essential point is that only those chains (or loops) bigger than s can reach the height $z(s)$, so the effective grafting density is $\rho(z) = D^>(s)$. This immediately gives $c(z) \approx D^{>2/3}(s)$, $z(s) = \int_0^s \text{d}s'D^{>1/3}(s')$ and brush height $h = \int_0^N \text{d}s D^>(s)$.

For the present structure we have $D^>(s) \approx s^{-1/2}$ for large loops $s \gg s^*$ and $D^>(s) \approx s^{*-1/2}$ for $s \ll s^*$, valid provided $s^* \ll N$. Thus

$$c(z) \approx \begin{cases} 1/z^{*2/5} = (\Gamma_{\text{tot}}/h)(h/z^*)^{2/5}, & z < z^*, \\ [5pt]1/z^{2/5} = (\Gamma_{\text{tot}}/h)(h/z)^{2/5}, & z > z^*, \end{cases} \quad z^* \equiv (Qt_{\text{final}})^{-5/3}, \qquad (8)$$

where $t_{\text{final}} \leq Q^{-1}$. Here $\Gamma_{\text{tot}} = \int_0^\infty \text{d}s s\Omega_t(s) \approx N^{1/2}$ is the total adsorbed mass per site and $z^* \equiv z(s^*) = s^{*5/6}$. This profile, sketched in fig. 1(c), has two distinct regions: 1) The inner region of total mass $\Gamma_{\text{inner}} = \Gamma_{\text{tot}}(s^*/N)^{1/2} \sim 1/t_{\text{final}}$, a small fraction of the total, has constant density $c_{\text{inner}} = \Gamma_{\text{inner}}/z^* \sim t_{\text{final}}^{2/3}$ up to z^*. 2) The more diffuse outer part, from z^* to the brush height $h = N^{5/6}$, where density decays as $z^{-2/5}$. This latter is the same decay as for Guiselin's physisorbed brush. Thus as the chemisorption experiment is interrupted at later and later times t_{final}, the inner region becomes progressively thinner and disappears at $t_{\text{final}} \approx 1/Q$. The blob structure is shown schematically in fig. 2(b).

Partially functionalised chains. – When a fraction f of chain units are chemically reactive ($f = 1$ was considered so far), there are now 2 monomer species whose relative affinity for the surface is an essential new parameter. Suppose there is an energy penalty ϵ when a reactive monomer displaces an unreactive one adjacent to the surface. Here we restrict attention to weakly repulsive or attractive surfaces, $|\epsilon| < kT$.

In the simplest case of a *neutral* surface ($\epsilon = 0$) most of the previous discussion is unchanged, provided one replaces $Q \to fQ$ and the loop cascade is truncated at $s_{\min} = f^{-1}$ at the corresponding loop lifetime, *i.e.* at $t_{\text{final}} = 1/(Qf^{1/2})$ (see eq. (4)). That is, after coarse-graining over scales $s_{\min}$ one recovers the case of 100% functionalization, but with reduced effective reactivity Qf. The final loop density is $\Gamma_{\text{bound}}^{\text{final}} = 1/s_{\min}^{1/2}$ and the swollen Guiselin brush is essentially unchanged, except that z^* reaches a minimum value $s_{\min}^{5/6}$ for long chemisorption times.

This is actually a slight simplification; $\Gamma_{\text{bound}}^{\text{final}}$ cannot be the true total surface loop density as $t \to \infty$, since the irreversibility of these reactions means that ultimately surface coverage must reach unity, $\Gamma_{\text{bound}} \to 1$. However, beyond t_{final} further coverage requires bringing down larger loops above their critical density. We find the consequent stretching energy penalty leads to exponentially suppressed reaction rates [19,20] and a slow logarithmic saturation $\Gamma_{\text{bound}} \approx \Gamma_{\text{bound}}^{\text{final}} \ln^{1/2}(t/t_{\text{final}})$. Thus for very large reaction times we predict the inner constant-density region ($z < z^*$) of the swollen brush will shrink and eventually disappear.

Consider now a surface weakly attractive to the reactive monomers, $\epsilon < 0$. Their tendency to preferentially physisorb prior to the much slower process of chemisorption is then weak; the entropic disadvantage (giving free-energy cost of order kT) of immobilization at the surface is not worth the energy gain. Similar remarks apply to weakly repulsive surfaces. In either case, the phenomenology is unchanged from the neutral case after replacing $Q \rightarrow Q e^{-\epsilon/kT}$.

Let us also consider the more complex situations where only a fraction X of chains are functionalised, beginning with neutral surfaces. The early stages of chemisorption now entail $\approx XQt$ single chains adsorbing independently, each producing $L(t)$ loops of size $s^*(t)$ as described by eq. (5) and preceding text. The net loop density is $\Gamma_{\text{bound}} \approx XQtL(t) \sim t^3$ reaching criticality when loops of size XN have descended after time $t_{\text{sat}} = Q^{-1}(XN)^{-1/2}$. The surface layer of thickness $(XN)^{1/2}$ is saturated and adsorption of new chains then essentially halts. The swelling experiment produces a Guiselin-type brush as described previously, but with N replaced by XN. Incomplete functionalization, $f < 1$, is dealt with as before.

Non-neutral surfaces are more complex because segregation effects now play a crucial role. A mean-field estimate of the energy of a chain close to the surface is proportional to the number of unperturbed surface contacts $N^{1/2}$ times the probability a given contact is a reactive monomer, $\Delta E \approx f N^{1/2} \epsilon$. When this is below kT, *i.e.* $f < f_{\text{crit}} = N^{-1/2}(kT/\epsilon)$, the neutral surface phenomenology is unmodified. For more heavily functionalised chains, chain configurations are strongly perturbed. This case will be discussed in ref. [14].

Topological constraints. – We end with a few remarks on how layer formation kinetics are interfered with by topological constraints, frozen in as interwoven loops are grafted to the surface. Thus far, such effects were neglected. Consider, for simplicity, $f = 1$ and neutral surfaces. At time t, the layer is a network of grafted loops with characteristic length $s^*(t)$. This network, bathed in a "solvent" of ungrafted free chains, has monomer density $\phi_{\text{net}} \approx \Gamma_{\text{bound}} s^{*1/2} \approx NX/s^*$. Thus, we expect topological constraints to be unimportant provided $s^* < N_e$, where $N_e = N_e^{\text{melts}}/\phi_{\text{net}}^{\gamma}$ is the entanglement threshold associated with this density. Here γ is an empirical system-dependent exponent [21] and N_e^{melts} the value in the melt. Insisting on this condition at all stages during layer formation (from $s^* = N$ at $t = 0$ to $s^* = XN$ at saturation), we conclude that provided $N < N_e^{\text{melts}}/X$ (if $\gamma > 1$) or $N < N_e^{\text{melts}}/X^{\gamma}$ (if $\gamma < 1$) then loops can always explore all configurations and loop rate constants $k(s \mid s')$ are governed by Gaussian statistics as assumed in our picture. If this condition is satisfied, topological constraints are irrelevant even after saturation, $t > t_{\text{sat}}$, since s^* then continues to decrease while the monomer density of the non-frozen part of the network ($s \leq s^*$) remains unity. Hence this part remains unentangled.

In summary, topological constraints do not interfere with the layer kinetics, provided either i) the melt is unentangled or ii) if the melt is entangled, the reactive chain fraction X must be small enough, $X < N_e^{\text{melts}}/N$ (taking a typical value $\gamma = 1$). The local reaction rate Q must also be small enough to allow exploration of all chain configurations before inhibition by further reactions. Noting an unreacted loop of length N makes of order $N^{1/2}$ surface contacts, the condition is $QN^{1/2}T_N < 1$, where $T_N \sim N^2$ is the loop Rouse relaxation time (for unentangled melts [18]) or $T_N \sim N^5$ (for entangled melts where loops relax via constraint release [21]). If the conditions on N and X are not satisfied, then no matter how small Q at a certain stage the entire layer freezes on scales large enough to be entangled (with the exception of tails which can relax via arm retraction mechanisms [18]). These situations will be discussed in a forthcoming publication [14].

Conclusions. – We have shown that slow formation of an adsorbed surface layer from a melt leads to a modified version of the Guiselin brush after swelling with solvent. In fact if the

adsorption process is allowed to proceed to completion ($t_{\text{final}} \to \infty$) the density profile of the swollen brush is unchanged from that predicted by Guiselin for instantaneous adsorption. For general interruption times t_{final}, there appears a new inner region of constant density whose width depends on t_{final}.

We have shown that reactions produce a characteristic loop distribution at the surface consisting of two power laws for small and large loops, respectively, with the dividing loop size s^* dependent on t_{final}. Our analysis describes systems where some or all chain units attach irreversibly to a surface but require many collisions to "cement in" these attachments. This is important in many applications involving chemisorption where the polymer loops created by surface reactions serve as bridges enhancing interfacial fracture toughness and yield stress after cooling [6–10]. The resulting interfacial strength depends strongly on loop size distributions [11, 22].

$$* * *$$

REFERENCES

[1]   Guiselin O., *Europhys. Lett.*, **17** (1992) 225.
[2]   Auvray L., Auroy P. and Cruz M., *J. Phys. I*, **2** (1992) 943.
[3]   Auvray L., Cruz M. and Auroy P., *J. Phys. II*, **2** (1992) 1133.
[4]   Durning C. J., O'Shaughnessy B., Sawhney U., Nguyen D., Majewski J. and Smith G. S., *Macromolecules*, **32** (1999) 6772.
[5]   Marzolin C., Auroy P., Deruelle M., Folkers J. P., Léger L. and Menelle A., *Macromolecules*, **34** (2001) 8694.
[6]   Kraus G., *Reinforcement of Elastomers* (John Wiley & Sons, New York) 1965.
[7]   Wu S., *Polymer Interface Adhesion* (Marcel Dekker, New York) 1982.
[8]   Edwards D. C., *J. Mater. Sci.*, **25** (1990) 4175.
[9]   Clegg D. W. and Collyer A. A. (Editors), *Mechanical Properties of Reinforced Thermoplastics* (Elsevier, London) 1986.
[10] Pireaux J. J., Bertrand P. and Bredas J. L. (Editors), *Polymer-Solid Interfaces* (Institute of Physics Publishing, Bristol) 1992.
[11] Creton C., Kramer E. J., Brown H. R. and Hui C.-Y., *Adv. Pol. Sci.*, **156** (2001) 53.
[12] Thon N. (Editor), *Tables of Chemical Kinetics. Homogeneous Reactions* (National Bureau of Standards, Department of Commerce) 1951.
[13] O'Shaughnessy B. and Vavylonis D., *Eur. Phys. J. E*, **11** (2003) 213 (cond-mat/0301206).
[14] O'Shaughnessy B. and Vavylonis D., in preparation.
[15] Shaffer J. S. and Chakraborty A. K., *Macromolecules*, **26** (1993) 1120.
[16] O'Shaughnessy B. and Vavylonis D., *Phys. Rev. Lett.*, **90** (2003) 056103.
[17] Semenov A. N. and Joanny J.-F., *Europhys. Lett.*, **29** (1995) 279.
[18] de Gennes P. G., *Scaling Concepts in Polymer Physics* (Cornell University Press, Ithaca, New York) 1985.
[19] O'Shaughnessy B. and Sawhney U., *Phys. Rev. Lett.*, **76** (1996) 3444.
[20] O'Shaughnessy B. and Sawhney U., *Macromolecules*, **29** (1996) 7230.
[21] Viovy J. L., Rubinstein M. and Colby R. H., *Macromolecules*, **24** (1991) 3587.
[22] Léger L., Raphaël E. and Hervet H., *Adv. Polym. Sci.*, **138** (1999) 185.